The Bisphosphonate Olpadronate Inhibits Skeletal Prostate Cancer Progression in a Green Fluorescent Protein Nude Mouse Model

Meng Yang,[1] Doug W. Burton,[2] Jack Geller,[1] Darren J. Hillegonds,[5] Randolph H. Hastings,[3] Leonard J. Deftos,[2] and Robert M. Hoffman[1,4]

Abstract

Purpose: Metastatic bone disease is one of the major causes of morbidity and mortality in prostate cancer patients. Bisphosphonates are currently used to inhibit bone resorption and reduce tumor-induced skeletal complications. More effective bisphosphonates would enhance their clinical value.

Experimental Design: We tested several bisphosphonates in a green fluorescent protein (GFP)–expressing human prostate cancer nude mouse model. The *in vivo* effects of four bisphosphonates, including pamidronate, etidronic acid, and olpadronate, on bone tumor burden in mice intratibially inoculated with PC-3-GFP human prostate cancer cells were visualized by whole-body fluorescence imaging and X-ray.

Results: The PC-3-GFP cells produced extensive bone lesions when injected into the tibia of immunocompromised mice. The skeletal progression of the PC-3-GFP cell growth was monitored by GFP fluorescence and the bone destruction was evaluated by X-ray. We showed that 3,3-dimethylaminopropane-1-hydroxy-1,1-diphosphonic acid (olpadronate) was the most effective bisphosphonate treatment in reducing tumor burden as assessed by GFP imaging and radiography. The GFP tumor area and X-ray score significantly correlated. Reduced tumor growth in the bone was accompanied by reduced serum calcium, parathyroid hormone–related protein, and osteoprotegerin.

Conclusions: The serum calcium, parathyroid hormone–related protein, and osteoprotegerin levels were significantly correlated with GFP area and X-ray scores. Treatment with olpadronate reduced tumor growth in the bone measured by GFP and X-ray imaging procedures. Imaging of GFP expression enables monitoring of tumor growth in the bone and the GFP results complement the X-ray assessment of bone disease. The data in this report suggest that olpadronate has potential as an effective inhibitor of the skeletal progression of clinical prostate cancer.

Prostate cancer is the most prevalent cancer in adult males. Despite increasing efforts at early detection, 10% to 20% of the patients will show metastases at the time of diagnosis (1, 2). Bone is a common site of prostate cancer metastases and bone metastases are responsible for most of the morbidity associated with this disease, such as bone pain and fractures (1, 2). The tendency of prostate cancer to spread to the skeleton indicates that tumor cells favor growth in bone. Prostate cancer cells express many factors that regulate osteoblasts and osteoclasts, including parathyroid hormone–related protein (PTHrP) and osteoprotegerin (3–5). PTHrP was originally discovered as the causative agent that is secreted by malignancies that results in hypercalcemia. PTHrP acts as a growth regulator of many different cell types and studies by us and our colleagues have shown that PTHrP regulates prostate tumor development, growth, progression, and metastasis (4). Osteoprotegerin is a potent inhibitor of bone resorption *in vivo* and is expressed by prostate cancer cells. Osteoprotegerin acts as a decoy receptor, binding and inactivating the receptor activator of nuclear factor-κB ligand, which is an essential factor required for osteoclast differentiation (5). The effects of these factors may explain, in part, the ability of prostate cancer cells to interact with the bone environment. Furthermore, these factors might serve as prognostic indicators for the risk of bone metastasis or as a measure of the extent of the metastasis.

Bisphosphonates are currently used as bone-specific palliative treatments to reduce skeletal complications from tumors that metastasize to bone. Many studies have shown that administration of bisphosphonates is useful in treating prostate, breast, and lung cancer that metastasize to the

Authors' Affiliations: [1]AntiCancer, Inc.; [2]Medicine and [3]Anesthesiology, Veterans Administration San Diego Healthcare System and University of California; [4]Department of Surgery, University of California, San Diego, California; and [5]Lawrence Livermore National Laboratory, Livermore, California

Received 9/19/05; revised 12/8/05; accepted 1/12/06.

Grant support: Veterans Administration Merit Review grants, Lawrence Livermore National Laboratory, NIH grants DK-60586, AR47347, and ES-09227; Prostate Cancer Research and Education Foundation grant and Department of Defense Prostate Cancer Research Program award no. DAMD17-01-1-0016.

The costs of publication of this article were defrayed in part by the payment of page charges. This article must therefore be hereby marked *advertisement* in accordance with 18 U.S.C. Section 1734 solely to indicate this fact.

Note: M. Yang and D.W. Burton contributed equally to this work.

Requests for reprints: Robert M. Hoffman, AntiCancer, Inc., 7917 Ostrow Street, San Diego, CA 92111. Phone: 858-654-2555; Fax: 858-268-4175; E-mail: all@anticancer.com.

doi:10.1158/1078-0432.CCR-05-2050

skeleton (6–9). They also induce apoptosis (10), reduce cell adhesion (11), inhibit angiogenesis (12), and decrease cell proliferation in several prostate cancer cell lines (13, 14). As a result, these agents are playing an increasing role in the treatment of painful bone metastases (6, 7).

We previously investigated several prostate carcinoma–derived proteins with effects in bone as potential markers of skeletal progression in a murine model of prostate carcinoma (15). This previous study evaluated the effects of treatment with the bisphosphonate, pamidronate, in immunocompromised mice with tibial injection of prostate carcinoma cell xenografts, on skeletal tumor progression and levels of calcium, PTHrP, and osteoprotegerin (15). We used a PC-3 human prostate carcinoma cell line expressing green fluorescent protein (GFP) to facilitate the monitoring of skeletal progression along with radiography and measurement of serum tumor markers. The PC-3 cells produced extensive bone lesions when injected into the tibia of immunocompromised mice (15, 16). Pamidronate treatment reduced tumor burden as assessed at autopsy and by imaging and biomarkers. Imaging of GFP expression enabled real-time monitoring of tumor growth in the bone (17). In the present study, we used a similar approach to examine the *in vivo* efficacy of four bisphosphonates on bone tumor burden (18) in mice that were intratibially inoculated with PC-3-GFP human prostate cancer cells.

Materials and Methods

Cell culture. The wild-type PC-3 cells, originally isolated from a human prostate adenocarcinoma that had metastasized to the bone, were genetically engineered to express GFP using a retrovirus expression vector (15). The PC-3-GFP cells were grown in monolayer in RPMI 1640 supplemented with 5% fetal bovine serum and incubated in a humidified chamber at 37°C with 95% air and 5% CO_2.

Animals. Six-month-old male, immunocompromised NCR nude (*nu/nu*) mice were housed in a barrier filter room and fed Purina rodent chow *ad libitum*. Animal experiments were done in accordance with the Guidelines for the Care and Use of Laboratory Animals (NIH publication no. 85-23) under assurance number A3873-01.

Tumor implantation and experimental course. Subconfluent PC-3-GFP cells were freshly trypsinized, counted, and placed on ice immediately before injection. The mice were injected with 10^6 cells in 15 μL sterile PBS into the bone marrow of the right tibia using a 26-gauge needle and a Hamilton glass syringe. The left tibia served as the negative control. Two months after implantation, the mice were anesthetized, exsanguinated for blood collection, and sacrificed.

Serum was prepared from blood and transferred to clean microcentrifuge tubes and frozen for subsequent measurements of serum biomarkers. Mice were evaluated for tumor growth and mass by GFP expression and by X-rays to assess the formation of bone lesions (4, 15–17).

Treatment. The mice were treated with the following bisphosphonates (a gift from Henkel KGaA, Duesseldorf, Germany): (**P**), disodium salt of 3-amino-1-hydroxypropane-1,1-diphosphonic acid (disodium salt of pamidronic acid, pamidronate), water content 8.2% (Ben Venue Labs, Bedford, OH); (**E**), disodium salt of 1-hydroxyethane-1,1 diphosponic acid tetra hydrate (etidronic acid), water content 22.5%; (**O**), 3,3-dimethylaminopropane-1-hydroxy-1,1-diphosphonic acid (olpadronate; ref. 19); and (**B**), 1,1′-diphosphonopropane-2,3′-dicarbonic acid monohydrate, water content 5.8%. The bisphosphonates and vehicle control (PBS) were injected i.v. at 2.6 mmol/L into the tail vein (18-20 mice per group) in a volume of 250 μL PBS beginning 1 month before intratibial implantation of prostate cancer cells. Additional treatment was administered at the time of tumor implantation and at 30 days after tumor implantation. The mice tolerated the treatments without any observed adverse side effects.

Fluorescent imaging and analyses. High-magnification imaging of GFP-expressing tumors was carried out with a Leica fluorescent stereomicroscope, model LZ12, equipped with a 50 W mercury lamp. Whole-body imaging was carried out in a light box illuminated by blue light fiber optics (Lightools Research, Encinitas, CA) and imaged using a thermoelectrically cooled color CCD camera (Hamamatsu Photonics, Bridgewater, NJ). The fluorescent images were analyzed on a Dell computer equipped with a Pentium 4 processor, 512 MB RAM and Windows XP Pro operating system (Microsoft Corporation, Redmond, WA) using Image-Pro Plus 4.5.1 software (Media Cybernetics, Silver Spring, MD). The maximum and total green pixel intensity values were quantitated from the digitized images and the data were exported to Microsoft Excel 2000 (Microsoft) for analyses (15).

X-ray imaging and analyses. Skeletal X-rays were exposed with 40 keV for 20 seconds in an HP Faxitron 5000 series X-ray cabinet. The Kodak X-Omat TL films were processed in a Kodak film processor. The X-ray images of the mouse tibiae injected with PC-3 cells were quantitated visually using a 10× Deluxe loop objective by two observers. The semiquantitation scoring method was formulated as 0, no lesions; 1, minor changes; 2, small lesions; 3, significant lesions (minor peripheral margin breaks, 1% to 10% of bone surface disrupted); 4, significant lesions (major peripheral margin breaks, >10% of bone surface disrupted; ref. 15).

Calcium, PTHrP, and osteoprotegerin measurement. Serum calcium was determined by the reaction of calcium with *o*-cresolphthalein to produce a red complex at pH 10 (Sigma Chemical, St. Louis, MO). The plates were scanned in a plate reader at a wavelength of 570 nm. A reference standard curve was also generated to convert the sample absorbance values into calcium concentrations (15). The mice sera were measured for PTHrP by RIA (4, 15). In brief, human PTHrP 38-64 peptide was used as standard and PTHrP 1-86 peptide was radioiodinated by the chloramine T method. Rabbit antiserum to PTHrP 38-64 was used in 3-day nonequilibrium immunoassay format. The limit of assay sensitivity was 4 pmol/L.

The osteoprotegerin immunoassay used antibodies purchased from R&D Systems (Minneapolis, MN; ref. 15). The two-site immunoassay was detected with a streptavidin-labeled β-D-galactosidase enzyme reaction using the fluorescent substrate, 4-methylumbelliferyl-β-D-galactopyranoside (Calbiochem, San Diego, CA) and had an assay sensitivity of 9 pg/mL. The human osteoprotegerin immunoassay kit (DY805) does not cross-react with mouse osteoprotegerin (R&D Systems).

Statistics. Statistical analyses were done using Microsoft Excel (Microsoft) and Statview (SAS, Cary, NC) software. Differences among treatment groups were assessed using ANOVAs and two-tailed Student's *t* tests. Correlation coefficient significance was determined using Documenta Geigy Scientific Tables, 6th edition. The X-ray scoring differences were tested using Kruskall-Wallis ANOVA and the Dunn test for *post hoc* analyses. $P < 0.05$ was considered to be statistically significant. Data are reported as mean ± SE.

Results

Evaluation of tumor masses and bone lesions. Fluorescent images taken 8 weeks after implantation of the PC-3-GFP cells into the right tibiae showed large tumors, >1 cm^3, in 18 of 20 of the control animals, 11 of 15 in the pamidronate-treated group (**P**), 15 of 18 in the etidronate-treated animals (**E**), and 18 of 19 in the bisphosphonate-B-treated mice (**B**). In contrast, the olpadronate-treated mice (**O**) did not show any tumors >1 cm^3 in volume.

X-ray analyses also showed severe osteolytic lesions in the majority of the control and pamidronate-, etidronate- and

bisphosphonate-B-treated mice, although some animals in each treatment group had no apparent bone abnormality. X-ray analyses of the olpadronate-treated mice confirmed the fluorometric images and showed 8 of 19 mice with no abnormalities and 11 of 19 with only minor abnormalities. No X-ray abnormalities were observed for the control tibiae or other areas of the skeleton in any of the mice. Examples of the typical fluorescent images and X-rays of the mice skeletons from the five groups are shown in Fig. 1.

The mice that were treated with pamidronate and olpadronate showed significant reduction ($P < 0.05$) in GFP area in the tibia as determined by pixel number compared with the control treated mice (Fig. 2). The pamidronate treatment group had a 52% reduction in GFP tumor area ($P < 0.05$), whereas the olpadronate-treated mice had a 66% decrease in the GFP tumor area compared with the GFP tumor area in the control mice ($P < 0.05$). No significant changes in GFP tumor area measurements were observed between the control and etidronate or bisphosphonate-B treatment groups (Table 1).

The severity of the bone lesions were quantitated by X-rays (Fig. 3). The mice that were treated with pamidronate showed a slight reduction in the severities of the bone lesions compared with the control-treated mice but it was not significant. The olpadronate-treated mice showed a dramatic reduction in the severity of the bone lesions compared with control mice ($P < 0.05$). Furthermore, the reduction in the X-ray scores for the olpadronate-treated group was significantly decreased compared with the pamidronate-treated group ($P < 0.05$). In fact, 17 of 19 mice in the olpadronate group had X-ray scores <1 and 8 of 19 mice had no observable tibial abnormalities. No significant changes in X-ray scores were observed between the control and etidronate- and bisphosphonate-B-treated mice (Table 1). The GFP tumor area and X-ray score results were significantly correlated ($r = 0.720$, $P < 0.01$).

Serum calcium, PTHrP, and osteoprotegerin levels. The serum calcium, PTHrP, and osteoprotegerin from the nontreated PC-3-GFP tumor-bearing mice were significantly elevated (serum calcium, mean ± SE = 14.6 ± 0.3 mg/dL; serum PTHrP, mean ± SE = 182 ± 13 pg/mL; and serum osteoprotegerin, mean ± SE = 282 ± 66 pg/mL) compared with non–tumor-bearing mice (serum calcium, mean ± SE = 10.3 ± 0.5 mg/dL; serum PTHrP, mean ± SE = 104 ± 9 pg/mL; and serum osteoprotegerin, mean ± SE = 31 ± 9 pg/mL; Table 1).

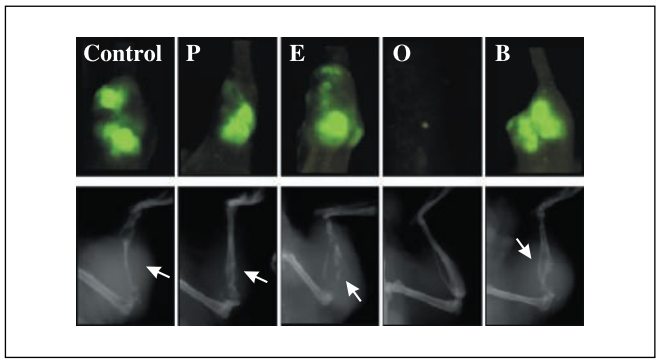

Fig. 1. Representative fluorescent (*top*) and X-ray (*bottom*) images of mouse tibia implanted with PC-3-GFP and treated with vehicle control or bisphosphonates. Typical images from the five groups of mice are shown: (*Control*) vehicle control – treated, (*P*) pamidronate, (*E*) etidronic acid, (*O*) 3,3′-dimethylaminopropane-1-hydroxy-1,1-diphosphonic acid (olpadronate), and (*B*) 1,1′-diphosphonopropane-2,3-dicarbonic acid monohydrate. Arrows, bone lesions. Note the significant decrease in the GFP fluorescence in the olpadronate- and pamidronate-treated mice and the reduction in the severity of the bone lesions in the olpadronate-treated group compared with the control and treated groups.

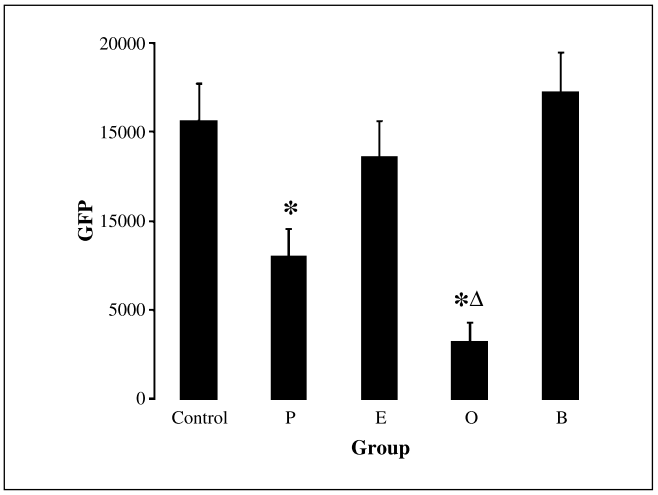

Fig. 2. GFP fluorescence shows that mice treated with olpadronate and pamidronate reduced skeletal tumor size. The graph plots the area of GFP fluorescence of the fluorescent images of the mouse right hind leg injected with PC-3-GFP cells. The tumor areas were determined using the sum of the pixel intensities. Olpadronate treatment caused a dramatic reduction in the GFP area compared with vehicle control and all other treatment groups. Columns, area of GFP fluorescence; bars, SE. *, $P < 0.05$ versus vehicle control, △, $P < 0.05$ versus pamidronate treatment.

Figure 4 and Table 1 show that there were no significant changes in serum calcium observed between the bisphosphonate treatment groups compared with the tumor-bearing control group except for the olpadronate-treated mice, which had serum calcium levels of 10.7 ± 0.4 mg/dL ($P < 0.05$).

The pamidronate- and olpadronate-treated mice showed significant decreases in serum PTHrP levels ($P < 0.05$) compared with the nontreated PC-3-GFP tumor-bearing mice (Fig. 4; Table 1). The olpadronate-treated mice were the only animals that showed a significant decrease in serum osteoprotegerin levels ($P < 0.05$) compared with the nontreated PC-3-GFP tumor-bearing mice (Fig. 4; Table 1). The serum calcium levels were significantly correlated with the GFP tumor area and X-ray scores ($r = 0.331$, $P < 0.01$ and $r = 0.461$, $P < 0.01$, respectively). The serum PTHrP and osteoprotegerin levels correlated with serum calcium levels ($r = 0.492$, $P < 0.01$ and $r = 0.495$, $P < 0.01$, respectively). The serum PTHrP and osteoprotegerin levels correlated with the GFP tumor areas ($r = 0.277$, $P < 0.01$ and $r = 0.344$, $P < 0.01$, respectively) and X-ray scores ($r = 0.584$, $P < 0.01$ and $r = 0.512$, $P < 0.01$, respectively), demonstrating their importance as biomarkers for the prostrate cancer tumor mass and bone destruction.

Discussion

As we have shown previously, our osseous-prostate cancer model, consisting of direct injection of GFP-expressing human prostate cancer cells into tibiae, is a useful tool for studying the effects of bisphosphonates on the skeletal progression of prostate cancer (15). This model provides a

Table 1. Efficacy of bisphosphonates on skeletal tumor growth, bone lesion severity, and serum biomarkers

Treatment	GFP tumor score (pixels)	X-ray score (0-4)	Serum calcium (mg/dL)	Serum PTHrP (pg/mL)	Serum OPG (pg/mL)
Control (non – tumor bearing)	0	0	10.3 ± 0.5	104 ± 9	31 ± 9
Control (tumor bearing)	15,626 ± 2,080	3.0 ± 0.3	14.6 ± 0.3	182 ± 13	282 ± 66
Bisphosphonate **P**	8,014 ± 1,591*	2.7 ± 0.2	13.0 ± 0.7	138 ± 8*	151 ± 29
Bisphosphonate **E**	12,861 ± 2,100	2.6 ± 0.4	13.8 ± 0.8	145 ± 14	176 ± 42
Bisphosphonate **O**	3,214 ± 1,109*	0.9 ± 0.2*	10.7 ± 0.4*	110 ± 6*	58 ± 22*
Bisphosphonate **B**	16,924 ± 2,256	3.4 ± 0.2	13.2 ± 0.8	197 ± 18	150 ± 32

Abbreviation: OPG, osteoprotegerin.
NOTE: Tumor area was measured by GFP imaging. The tibial lesion severity was determined by X-ray. Serum biomarkers were measured as described in the Materials and Methods. Values are the mean ± SE. The *P* values are based on two-tailed Student's *t* tests and are compared with the control (tumor-bearing) group.
*$P < 0.05$.

reliable method for producing prostate carcinoma xenografts in bone where GFP imaging can monitor tumor progression in real time. The X-ray and GFP scores of the skeletal prostate cancer significantly correlated with each other. Both measurements are useful in quantifying the tumor mass. X-ray imaging is useful for the determination of the severity of the bone lesion. Serum calcium, PTHrP, and osteoprotegerin measurements correlated with the GFP tumor area and X-ray scores and provide additional information to monitor tumor progression. There were important differences in the responses of the prostate cancer tumor-bearing mice to the various bisphosphonate treatments. Only the olpadronate- and pamidronate-treated mice showed significant improvements in reducing the tumor growth and the severity of the tibial lesions compared with the nontreated tumor-bearing mice. Olpadronate treatment reduced both tumor mass and the severity of the bone lesions and showed corresponding decreases in serum calcium, PTHrP, and osteoprotegerin. Pamidronate treatment reduced the tumor mass but had no effect on the severity of the bone lesions. The X-rays of the olpadronate-treated mice clearly showed a reduction in bone destruction in the injected tibiae compared with the other bisphosphonate-treated mice. We did not include histology of the tumor deposits to confirm our conclusions because the differences were so dramatic. The serum biomarkers in the pamidronate-treated mice showed significant decreases in PTHrP levels but no changes in calcium or osteoprotegerin levels compared with the levels in the nontreated tumor-bearing mice. Thus, PTHrP seems to be a better marker for tumor mass whereas osteoprotegerin and calcium are more reflective of bone destruction.

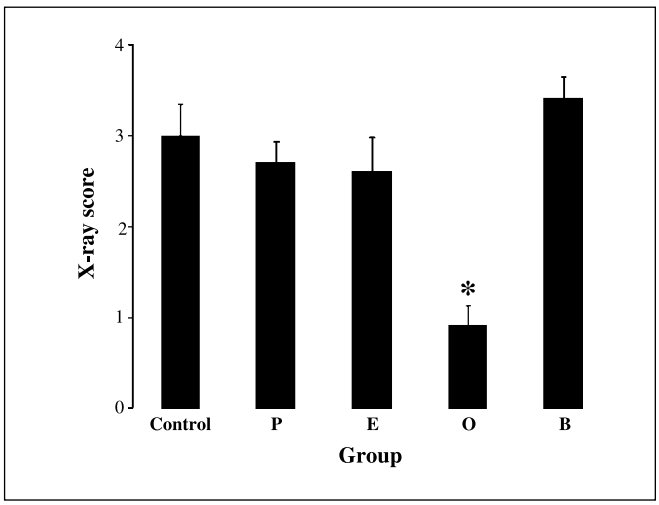

Fig. 3. X-ray scores of mouse tibiae show that olpadronate decreased the severity of bone lesions compared with control mice. The X-ray images of the mouse tibiae injected with PC-3-GFP cells were evaluated by two observers and assigned a score. The semiquantitative scoring method was formulated as 0, no lesions; 1, minor changes; 2, small lesions; 3, significant lesions (minor peripheral margin breaks, 1% to 10% of bone surface disrupted); 4, significant lesions (major peripheral margin breaks, >10% of bone surface disrupted). Olpadronate treatment caused a much greater reduction in the severity of the bone lesions above that seen with pamidronate. Columns, X-ray scores; bars, SE. *, $P < 0.05$ versus vehicle control.

A previous study on olpadronate by van der Pluijm et al. (19) was a time course study on bone lesions in mice from a human breast tumor using luciferase imaging and radiography. However, there were discrepancies in the luciferase imaging and radiography, making the results of bisphosphonate efficacy difficult to interpret. In contrast, GFP imaging and radiography correlated in our study indicating that olpadronate inhibited both osteolytic activity and tumor burden. The results of van der Pluijm et al. (19) may reflect problems with luciferase imaging. We did not perform real-time fluorometry in this study. Instead, we focused on the end-stage time point only because we initially wanted to compare the long-term effects of the bisphosphonates on the progression of the prostate cancer in bone and correlate the GFP, X-ray, and serum biomarkers. We plan to perform future time course studies and take advantage of the ability of real-time fluorescence imaging to assess tumor growth changes as a result of treatment modalities.

Bone metastases are common in prostate cancer and are a clinically relevant source of morbidity. Bisphosphonates are potent inhibitors of osteoclast activity and have shown efficacy in the treatment of bone metastases (20). Bisphosphonates bind avidly to the bone matrix, are released during bone resorption, and are subsequently internalized by osteoclasts, where they interfere with biochemical pathways and induce osteoclast apoptosis. Bisphosphonates also antagonize osteoclastogenesis and promote the differentiation of osteoblasts (7, 21). Preclinical studies suggested that

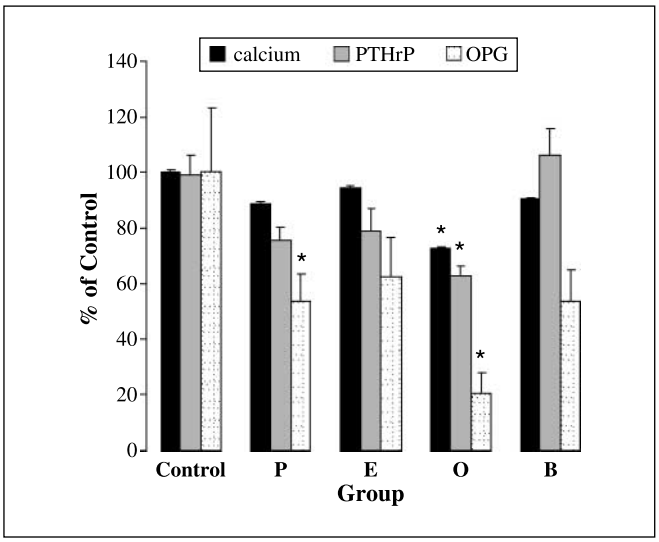

Fig. 4. Treatment with olpadronate decreases serum calcium, PTHrP, and osteoprotegerin compared with control mice. The mice were bled 8 weeks after injection of PC-3-GFP cells and the calcium, PTHrP, and osteoprotegerin levels were measured in the sera. Columns, percentage of control; bars, SE. *, $P < 0.05$, significant difference compared with the tumor-bearing control group based on two-tailed Student's t tests.

bisphosphonates possess antitumor activity and can inhibit proliferation and induce apoptosis of tumor cells (11, 14). Clinical trials investigating the benefit of bisphosphonate therapy have shown that pamidronate, etidronic acid, and other bisphosphonates significantly reduce the incidence of skeletal events in patients with bone metastases (7, 8, 22). In addition, zoledronic acid, a new generation bisphosphonate, seems to inhibit tumor cell invasion of the extracellular matrix by inhibiting osteoclast activity at the metastatic site (23). However, zoledronic acid treatment can result in renal failure (18). Therefore, work is ongoing to develop bisphosphonates with greater efficacy in reducing metabolic progression with fewer side effects. The most effective bisphosphonate in preventing bone destruction and tumor growth in our skeletal prostate cancer mouse model was olpadronate. Olpadronate is a nitrogenated bisphosphonate derived from pamidronate that is more potent and has a greater digestive tolerability than the other bisphosphonates tested in our study (24). Olpadronate was previously shown to be effective in reducing bone pain in a small clinical trial of patients with metastatic carcinoma of the prostate. The clinical response seemed to parallel decreases in urinary calcium and hydroxyproline excretion but no correlations were made to skeletal progression (25).

In summary, our *in vivo* mouse model for prostate cancer metastasis using GFP imaging, X-rays, and biomarkers provides a reliable method for screening the efficacy of treatment modalities for prostate cancer. In our study, mice treated with olpadronate showed a dramatic reduction in the severity of the bone lesion and inhibition of the growth of the prostate cancer tumor, as assessed by X-ray and GFP imaging, respectively. Thus, olpadronate shows promise for clinical use and additional studies are warranted.

References

1. Karayi MK, Markham AF. Molecular biology of prostate cancer. Prostate Cancer Prostatic Dis 2004; 7:6–20.
2. Bubendorf L, Schopfer A, Wagner U, et al. Metastatic patterns of prostate cancer: an autopsy study of 1,589 patients. Hum Pathol 2000;31:578–83.
3. Wu G, Iwamura M, di Sant'Agnese PA, Deftos LJ, Cockett AT, Gershagen S. Characterization of the cell-specific expression of parathyroid hormone-related protein in normal and neoplastic prostate tissue. Urology 1998;51:110–20.
4. Deftos LJ, Barken I, Burton DW, Hoffman RM, Geller J. Direct evidence that PTHrP expression promotes prostate cancer progression in bone. Biochem Biophys Res Commun 2005;327:468–72.
5. Brown JM, Corey E, Lee ZD, et al. Osteoprotegerin and RANK ligand expression in prostate cancer. Urology 2001;57:611–6.
6. Chung LW, Baseman A, Assikis V, Zhau HE. Molecular insights into prostate cancer progression: the missing link of tumor microenvironment. J Urol 2005;173:10–20.
7. Ross JR, Saunders Y, Edmonds PM, et al. A systematic review of the role of bisphosphonates in metastatic disease. Health Technol Assess 2004;8:1–176.
8. Saad F, Gleason DM, Murray R, et al. Zoledronic Acid Prostate Cancer Study Group. A randomized, placebo-controlled trial of zoledronic acid in patients with hormone refractory metastatic prostate carcinoma. J Natl Cancer Inst 2002;94:1458–68.
9. Zhang H, Yano S, Miki T, et al. A novel bisphosphonate minodronate (YM529) specifically inhibits osteolytic bone metastasis produced by human small-cell lung cancer cells in NK-cell depleted SCID mice. Clin Exp Metastasis 2003;20:153–9.
10. Conte PF, Latreille J, Mauriac L, et al. Delay in progression of bone metastases in breast cancer patients treated with intravenous pamidronate: results from a multinational randomized controlled trial. The Aredia Multinational Cooperative Group. J Clin Oncol 1996; 14:2552–9.
11. Hughes DE, Wright KR, Uy HL, et al. Bisphosphonates promote apoptosis in murine osteoclasts *in vitro* and *in vivo*. J Bone Miner Res 1995;10:1478–87.
12. van der Pluijm G, Vloedgraven H, van Beek E, van der Wee Pals L, Lowik C, Papapoulos S. Bisphosphonates inhibit the adhesion of breast cancer cells to bone matrices *in vitro*. J Clin Invest 1996;98:698–705.
13. Fournier P, Boissier S, Filleur S, et al. Bisphosphonates inhibit angiogenesis *in vitro* and testosterone-stimulated vascular regrowth in the ventral prostate in castrated rats. Cancer Res 2002;62:6538–44.
14. Lee MV, Fong EM, Singer FR, Guenette RS. Bisphosphonate treatment inhibits the growth of prostate cancer cells. Cancer Res 2001;61:2602–8.
15. Burton DW, Geller J, Yang M, et al. Monitoring of skeletal progression of prostate cancer by GFP imaging, X-ray, and serum OPG and PTHrP. Prostate 2005; 62:275–81.
16. Yang M, Jiang P, Sun FX, et al. A fluorescent orthotopic bone metastasis model of human prostate cancer. Cancer Res 1999;59:781–6.
17. Hoffman RM. Green fluorescent protein imaging of tumour growth, metastasis, and angiogenesis in mouse models. Lancet Oncol 2002;3:546–56.
18. Chang JT, Green L, Beitz J. Renal failure with the use of zoledronic acid. N Engl J Med 2003;349:1676–9.
19. van der Pluijm G, Que I, Sijmons B, et al. Interference with the microenvironmental support impairs the *De novo* formation of bone metastasis *in vivo*. Cancer Res 2005;65:7682–90.
20. Xie A, Liao C, Li Z, et al. Quantitative-structure-activity relationship study of bisphosphonates. Internet Electron J Mol Des 2004;3:622–50.
21. Corey E, Brown LG, Quinn JE, et al. Zoledronic acid exhibits inhibitory effects on osteoblastic and osteolytic metastases of prostate cancer. Clin Cancer Res 2003;9:295–306.
22. Conte P, Coleman R. Bisphosphonates in the treatment of skeletal metastases. Semin Oncol 2004;31: 59–63.
23. Peyruchaud O, Serre CM, NicAmhlaoibh R, Fournier P, Clezardin P. Angiostatin inhibits bone metastasis formation in nude mice through a direct anti-osteoclastic activity. J Biol Chem 2003;278:45826–32.
24. Pelger RC, Hamdy NA, Zwinderman AH, Lycklama a Nijeholt AA, Papapoulos SE. Effects of the bisphosphonate olpadronate in patients with carcinoma of the prostate metastatic to the skeleton. Bone 1998;22: 403–8.
25. Widler L, Jaeggi KA, Glatt M, et al. Highly potent geminal bisphosphonates. From pamidronate disodium (Aredia) to zoledronic acid (Zometa). J Med Chem 2002;45:3721–38.

Clinical Cancer Research

The Bisphosphonate Olpadronate Inhibits Skeletal Prostate Cancer Progression in a Green Fluorescent Protein Nude Mouse Model

Meng Yang, Doug W. Burton, Jack Geller, et al.

Clin Cancer Res 2006;12:2602-2606.